Synthesis and Structural Characterization of Layered Cuprates Containing a Lead Halide Separating Layer

R. J. Crooks, C. S. Knee, and M. T. Weller*

Department of Chemistry, The University of Southampton, Southampton, SO17 1BJ

Received September 2, 1998. Revised Manuscript Received October 5, 1998

A series of layered cuprates of the general formula $Pb_y(Ba/Sr)_{4-y}Cu_2MO_8X$, where M = Nb, Ta, and Sb; X = Br and Cl; and $y = 2$, 3, have been synthesized. The detailed structural characterization of these materials has been performed using Rietveld refinement of high-resolution PND data. The compounds crystallize with a tetragonal unit cell, space group $P4/mmm$; cell parameters in the range $a = 3.8982(2)-3.9732(2)$ Å and $c = 15.3886(8)-15.8689(11)$ Å. The structure of the materials consists of two CuO_5 square pyramids connected by a $(Ba/Sr)MO_3$ perovskite layer, a unit also present in the widely studied Ln−1212 phases, with an interleaving Pb_2X layer. The material $Pb_2Sr_2Cu_2SbO_8Cl$ has the shortest Cu−O in plane bond length of 1.9570(5) Å, which lies close to the length required for the observation of superconductivity. However, preliminary investigation of the electronic properties of these materials show that they exhibit semiconducting behavior down to 4 K.

Introduction

Examination of the majority of high temperature (high-T_c) copper oxide superconductors indicates that there are several structural prerequisites for a material to exhibit superconductivity. These include linked copper oxide planes, containing copper in four (square planar), five (square based pyramidal), or six (octahedral) coordination, interspaced by a series of connecting or separating layers. New layered cuprates as potential high-T_c superconductors can therefore be envisaged by interleaving different combinations of the connecting and separating layers, as well as the copper oxide planes. A variety of separating layers has been observed in high-T_c materials. These layers frequently exist as rock salt blocks, e.g. BaO in $TlBa_2Cu_2Cu_3O_{9+\delta}$,[1] SrO in $(Tl,Pb)Sr_4Cu_2CO_3O_6$,[2] or LaO in $Pb_2(Sr,La)_2Cu_2O_6$.[3] Another separating layer occasionally seen in metal oxide systems has the stoichiometry "Pb_2Cl" adopting a CsCl type arrangement. Examples of materials containing this structural block include the mineral hematophanite, $Pb_4Fe_3O_8Cl$,[4] and the lead-based cuprate $Pb_3Sr_3Cu_3O_8Cl$.[5] Three materials containing these Pb_2Cl spacing layers, $Pb_2Ba_2Cu_2NbO_8Cl$, $Pb_2Ba_2Cu_2TaO_8Cl$,[6] and $Pb_2Sr_2Cu_2TaO_8Cl$,[7] have recently been reported by Li. The structures of these materials, determined from powder X-ray diffraction data, contain linked CuO_5 pyramids forming infinite sheets, connected by MO_6 octahedra between the Pb_2Cl layers.

In this paper we report the extension of this family of compounds with the synthesis and characterization of Sr and Br analogues of $Pb_2Ba_2Cu_2NbO_8Cl$ and $Pb_2Ba_2Cu_2TaO_8Cl$ and the new antimony derivatives $Pb_2(Ba/Sr)_2Cu_2SbO_8X$, X = Br and Cl. In addition, the lead-rich phases $Pb_3BaCu_2SbO_8X$, X = Cl and Br, and $Pb_3BaCu_2TaO_8Cl$ are reported. Structural characterization of the materials is performed primarily using Rietveld refinement of high-resolution powder neutron diffraction in order to determine accurately the structural features involving oxygen.

The structures of the various materials that can be synthesized in this system are compared and apparent trends discussed. Finally, comments regarding the likelihood of inducing superconductivity in this type of material are made.

Experimental Procedure

Synthesis. The materials were synthesized following the methods originally described by Li.[6] This involved the intimate mixing of PbO (99.9%), $PbBr_2$ (99.9%), $PbCl_2$ (99.9%), $Ba(NO_3)_2$ (99.9%), $Sr(NO_3)_2$ (99.9%), Ta_2O_5 (99.5%), Nb_2O_5 (99.5%), Sb_2O_5 (99.5%), and CuO (99.95%) in the appropriate stoichiometric amounts. The starting materials were then preheated to 550 °C and then 650 °C in air, for 12 h each, with intermediate regrinds. The resulting powders were again reground, pelletized (~8 tons/cm^2), and calcined in air at 700 °C for 24 h. The final heating procedure was repeated until no change in the powder X-ray diffraction pattern was observed. Table 1 provides a summary of the targeted phases, sample purity, and cell parameters, as determined from powder X-ray diffraction or powder neutron diffraction data.

Powder X-ray Diffraction Structure Refinement. Powder X-ray diffraction data were collected in the 2θ range 20−110° using a Siemens D5000 diffractometer (Cu Kα1 radiation), a step size of 0.02°, and a count time of 12 s/step. Structural refinement using the Rietveld method and GSAS

* Corresponding author: Phone and Fax: 00 44 1703 593592. E-mail mtw@soton.ac.uk.

(1) Parkin, S. S. S.; Lee, V. Y.; Nazzal, A. I.; Savoy, R.; Beyers, R.; LaPlaca, S. J. *Phys. Rev. Lett.* **1988**, *61*, 750.
(2) Huvé, M.; Michel, C.; Maignan, A.; Hervieu, M.; Martins, C.; Raveau, B. *Physica C* **1993,** *205*, 219.
(3) Benschop, F. J. M.; Fu, W. T.; Maaskant, W. J. A. *Physica C* **1991**, *184*, 311.
(4) Pannetier, J.; Batail, P. *J. Solid State Chem.* **1981**, *39*, 15.
(5) Cava, R. J.; Bordet, P.; Capponi, J. J.; Chaillout, C.; Chenavas, J.; Fournier, T.; Hewat, E. A.; Hodeau, J. L.; Levy, J. P.; Marezio, M.; Batlogg, B.; Rupp, L. W., Jr. *Physica C* **1990**, *167*, 67.
(6) Li, Rukang. *Physica C* **1997**, 277, 252.
(7) Li, Rukang. *J. Solid State Chem.* **1997**, *130*, 154.

10.1021/cm980609n CCC: $15.00
Published on Web 11/19/1998

Table 1. A Summary of the Phases Synthesized in the Series $Pb_y(Ba/Sr)_{4-y}Cu_2MO_8X$, y = 2, 3

target stoichiometry	cell parameters (Å)	impurity phase(s)
$Pb_2Ba_2Cu_2SbO_8Cl$	$a = 3.9585(3)$ $c = 15.6564(12)$	$BaPbO_3$, CuO
$Pb_2Ba_2Cu_2SbO_8Br$[a]	$a = 3.9521(8)$ $c = 15.858(5)$	CuO
$Pb_2Sr_2Cu_2SbO_8Cl$	$a = 3.8982(2)$ $c = 15.3886(8)$	CuO
$Pb_2Sr_2Cu_2SbO_8Br$	$a = 3.9067(2)$ $c = 15.6688(12)$	CuO
$Pb_2Ba_2Cu_2NbO_8Cl$[b]	$a = 3.9576(1)$ $c = 15.6063(13)$	CuO
$Pb_2Ba_2Cu_2NbO_8Br$	$a = 3.9732(2)$ $c = 15.8263(11)$	CuO
$Pb_2Sr_2Cu_2NbO_8Cl$[a]	$a = 3.8985(6)$ $c = 15.348(3)$	Sr_2PbO_4, CuO
$Pb_2Sr_2Cu_2NbO_8Br$[a]	$a = 3.9077(5)$ $c = 15.624(4)$	Sr_2PbO_4, CuO
$Pb_2Ba_2Cu_2TaO_8Cl$[b]	$a = 3.9531(1)$ $c = 15.6332(11)$	CuO
$Pb_2Ba_2Cu_2TaO_8Br$	$a = 3.9686(2)$ $c = 15.8689(11)$	$BaPbO_3$
$Pb_2Sr_2Cu_2TaO_8Cl$[b]	$a = 3.9004(3)$ $c = 15.4231(11)$	CuO
$Pb_2Sr_2Cu_2TaO_8Br$	$a = 3.9097(3)$ $c = 15.6912(20)$	CuO
$Pb_3BaCu_2TaO_8Cl$	$a = 3.9374(4)$ $c = 15.565(2)$	CuO
$Pb_3BaCu_2TaO_8Br$	unsuccessful	$BaPbO_3$, PbO, CuO
$Pb_3BaCu_2SbO_8Cl$[a]	$a = 3.9274(4)$ $c = 15.531(2)$	$BaPbO_3$ (∼10%), CuO
$Pb_3BaCu_2SbO_8Br$[a]	$a = 3.9404(4)$ $c = 15.760(2)$	$BaPbO_3$ (∼10%), CuO

[a] The material was characterized by PXD only. [b] The materials highlighted in bold are those previously reported by Li.[6,7]

program,[8] in the tetragonal space group *P4/mmm*, was then performed using these data sets. The atomic positions used as a starting point for the refinements were the coordinates reported for $Pb_2Ba_2Cu_2TaO_8Cl$ by Li[6] with the exception of the O1 oxygen site, whose position was erroneously reported as (0,0,0.21) rather than (0,0.5,0.21). Initial atomic coordinates were as follow: Pb, 2h (0.5,0.5,0.12); Ba/Sr, 2h (0.5,0.5,0.35); M, 1b (0,0,0.5); Cu, 2g (0,0,0.22); O1, 4i (0,0.5,0.21); O2, 2g (0,0,0.37); O3, 2e (0,0.5,0.5); and Cl/Br, 1a (0,0,0). See Figure 1. For the series $Pb_3BaCu_2MO_8X$, M = Sb and Ta, the additional lead was situated on the Ba site in a 50:50 ratio. The refinements proceeded smoothly with the introduction, where necessary, of minor impurity phases ($I/I_0 < 5\%$), and accurate lattice parameters and heavy atom coordinates were obtained for 15 samples. While the heavy atom positions were well defined in these refinements, the oxygen atomic and thermal parameters were poorly determined. Therefore 10 samples were chosen for further study using powder neutron diffraction.

Powder Neutron Diffraction Data. Eight of the samples were studied on the high-resolution constant wavelength powder neutron diffractometer D2B at the I.L.L, Grenoble. For two other materials, namely $Pb_2Ba_2Cu_2TaO_8Cl$ and $Pb_2Ba_2Cu_2NbO_8Cl$, data were collected on the high-resolution diffractometer HRPD on ISIS at the Rutherford Appelton Laboratory.

Collection of Data on D2B. A 3−4 g sample was placed in a 10 mm diameter vanadium can. The powder pattern was collected at steps of $2\theta = 0.025°$ over the range 5−165° on the high-resolution powder neutron diffractometer D2B ($\lambda = 1.594$ Å) over a time period of approximately 8 h at ambient temperature.

Collection of Data on HRPD. A 4 g sample was sealed in a 12 mm thin-walled vanadium can, and data were collected using the backscattering detectors, with the sample in the 1 m position, over a period of 8 h, at room temperature.

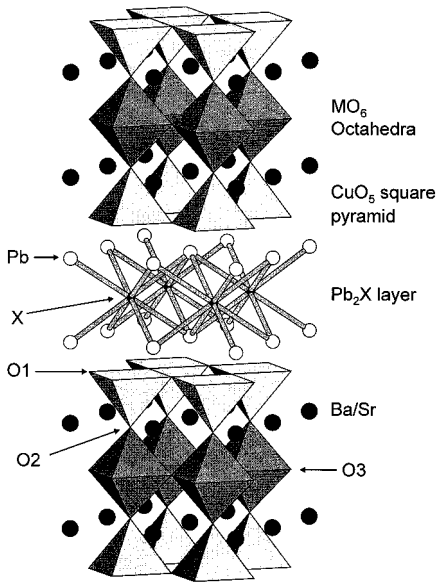

Figure 1. The structure of $Pb_2(Ba/Sr)_2Cu_2MO_8X$. The copper coordination is shown as a square based pyramid separated by MO_6 octahedra. The halide environment is shown bonding 8-fold to the lead atoms forming a Pb_2X layer.

Powder Neutron Diffraction Structure Refinement. The neutron powder diffraction patterns of the compounds were refined, again using the GSAS program[8] and the same starting structural model as previously described. The nuclear scattering lengths used were Pb = 9.400 fm, Ba = 5.250 fm, Sr = 7.020 fm, Cu = 7.718 fm, Nb = 7.050 fm, Ta = 6.910 fm, Sb = 5.640 fm, Br = 6.790 fm, Cl = 9.580 fm, and O = 5.805 fm.[9] Initial stages of the refinements included background parameters, histogram scale factor, peak shape, lattice parameters, and zero point displacement. Detailed inspection of the patterns revealed the presence in all data sets of a small level of CuO, and this was introduced into the refinements as a second phase using literature data.[10] Other minor impurity phases, e.g. $BaPbO_3$[11] were included where necessary. The refinement(s) proceeded with the introduction of atomic and isotropic thermal parameters for all the atoms. These refined to satisfactory values except for the oxygen site O3, which gave an unreasonably large value. The atom, which lies in the basal plane of the MO_6 octahedra, was therefore displaced from (0,0.5,0.5) onto a half-occupied 2-fold (x,0.5,0.5), $x \sim 0.1$, site. Similar disordering of oxygen, which probably represents a twisting or distortion of the MO_6 octahedra, has been found in other multilayer cuprate materials containing early transition metals.[12,13] This displacement refined steadily for all the samples resulting in the reduction of the temperature factor to an acceptable value and an improvement to the profile fit. The refined displacement was greater in the strontium-containing phases. For the refinement of the lead-rich phase $Pb_3BaCu_2TaO_8Cl$, the atomic coordinate and thermal parameter of the mixed Ba/Pb site were constrained together and both refined to give acceptable values. Finally, the fractional occupancies of the oxygen atoms were probed to check for any oxygen deficiency; however, they refined to unity with satisfactory thermal parameters.

Final profile fits obtained for $Pb_2Sr_2Cu_2SbO_8Cl$ run on D2B and $Pb_2Ba_2Cu_2TaO_8Cl$ run on HRPD are shown in Figures 2

(8) Larson, A. C.; Von Dreele, R. B. *MS-H805*; Los Alamos National Laborotory: Los Alamos, NM, 87545.

(9) Koester, L.; Rauch, H.; Seymann, E. *Atomic Nuclear Data Tables* **1991**, *49*, 65.

(10) Asbrink, S.; Lorrby, L. J. *Acta Crystallogr.* **1970**, *26B*, 8.

(11) Thornton, G.; Jacobson, A. J. *Mater. Res. Bull.* **1976**, *11*, 837.

(12) Rey, M. J.; Dehaudt, P.; Joubert, P.; Hewat, A. W. *Physica C* **1990**, *167*, **No**. 1−2, 162.

(13) Pack, M. J.; Gormezano, A.; Weller, M. T. *Chem. Mater.* **1997**, *9(7)*, 1547.

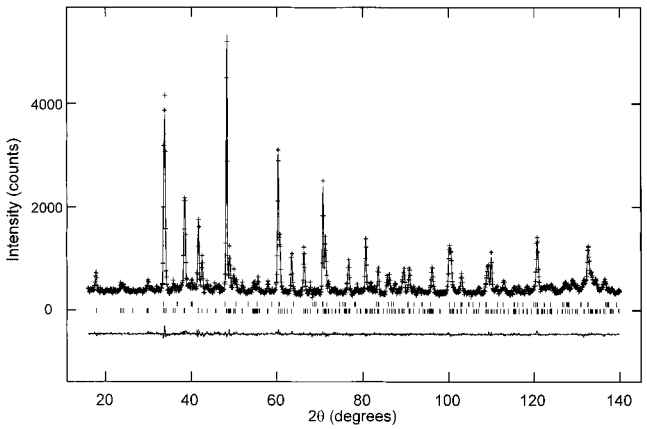

Figure 2. Final profile fit for $Pb_2Sr_2Cu_2SbO_8Cl$ run on the constant wavelength diffractometer D2B. Crosses mark observed intensities, the upper continuous line is the calculated profile, and the lower continuous line is the difference. Reflections are indicated with tick marks for $Pb_2Sr_2Cu_2SbO_8$-Cl (lower) and CuO (upper).

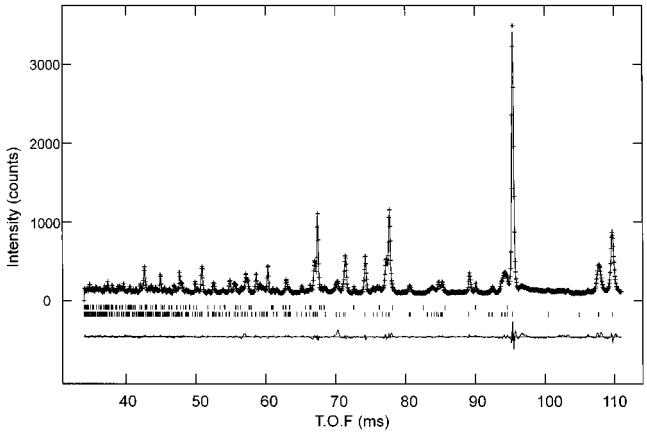

Figure 3. Final profile fit for $Pb_2Ba_2Cu_2TaO_8Cl$ run on the pulsed HRPD instrument. Crosses mark observed intensities, the upper continuous line is the calculated profile, and the lower continuous line is the difference. Reflections are shown with tick marks for $Pb_2Ba_2Cu_2TaO_8Cl$ (lower) and CuO (upper).

and 3. Cell parameters are shown in Table 1, refined atomic parameters summarized in Table 2, and derived bond lengths shown in Table 3.

Results and Discussion

The basic structure of the phases $Pb_2(Ba/Sr)_2Cu_2MO_8X$ is shown in Figure 1. A three-block perovskite unit, with the repeat $CuO_2{\cdot}(Ba/Sr)O{\cdot}MO_2{\cdot}(Ba/Sr)O{\cdot}CuO_2$, is separated by the Pb_2X layers. Changes in lattice parameters, particularly in the *c*-direction reflect those expected for the different ionic radii of the halide X and the alkali earth cations. The strontium-based materials have a distinctly lower *c*-parameter than those containing barium and also contract significantly in the *ab*-plane (~0.06 Å). Replacement of bromide by chloride as expected causes a marked contraction along the *c*-direction, but in this case the *a*-direction only decreases by about 0.015 Å. There are little differences in the accepted ionic radii of Nb^{5+} (0.64), Ta^{5+} (0.64), and Sb^{5+} (0.61 Å),[14] and the small variations in *a* and *c* observed for the different pentavalent ions reflect these values.

The in-plane copper−oxygen distances and the apical copper−oxygen distance are strongly affected by the size of the alkali earth atom, and the origin of the changes in the unit cell parameters can be seen from these variations. However, the buckling of the copper−oxygen planes remains relatively constant with the O1 oxygen atoms lying ~0.15 Å above/below the copper. In $Pb_2(Ba/Sr)_2Cu_2SbO_8Cl$ and $Pb_2(Ba/Sr)_2Cu_2TaO_8X$ replacing barium by strontium causes the equatorial copper−oxygen bond length to decrease by around 0.03 Å and the apical distance by around 0.10 Å. This would imply that occupation of the perovskitic A type cation site by barium places the copper−oxygen framework under considerable expansive stress, which is relieved with the smaller strontium**.** As the alkaline earth coordinates to O1 and O2, both copper−oxygen distances decrease markedly. Replacing the smaller chloride by bromide in the structure has little effect on the copper−oxygen distances, as these sections are well-separated from each other. The shortest Cu−O distances are thus found in $Pb_2Sr_2Cu_2SbO_8Cl$ and $Pb_2Sr_2Cu_2TaO_8Cl$, where the Cu−O separation drops to under 1.96 Å. This is close to the values expected in superconducting oxides, which are typically in the range 1.9−1.96 Å, though it is probably still too high to induce superconductivity, even if these materials could be appropriately doped.

An additional feature of this structure is the disorder in the $Nb/Ta/SbO_6$ layers. Similar structural disorder occurs in many multiple B cation perovskites and may result from either an incompatibility of the sizes of the cuprate and other B cation layers or may just be the result of this highly charged, strongly polarizing B′ cation. To obtain layered segregation of the different B type cations, the charges on them normally have to be significantly different;[15] in combination with copper 2+ this usually means B′ is 4+, 5+, or 6+. Such species often strongly polarize the MO_6 octahedra producing one shorter M−O distance or some other structural distortion. In these $Pb_2(Ba/Sr)_2Cu_2MO_8X$ phases this is modeled structurally by displacing the O3 ion from (0,0.5,0.5) to near (0.1,0.5,0.5). This distortion of the MO_6 in the *ab*-plane may explain the slightly lower than expected M thermal parameters obtained for some of the samples, in particular the Sb and Ta phases. It is noteworthy that the magnitude of this displacement is considerably less in all the barium derivatives studied than in the strontium-containing materials. The smaller strontium may require greater distortion or rotation of the octahedra to achieve a shorter Sr−O distances, but the decrease in *a*, caused by replacing barium by strontium, also requires greater rotation of the octahedra. This distortion of the octahedra (Figure 4) has the effect of lengthening the in-plane M−O distances for a fixed *a* lattice parameter; for example, in $Pb_2Sr_2Cu_2SbO_8Cl$ an O3 site of (0,0.5,0.5) would produce an Sb−O distance of 1.949 Å, but with the displacement this increases to just over 2.00 Å. This displacement is best modeled using a half-occupied site for O3. As no evidence for a supercell, caused by these octahedra rotations, was found, the refined oxygen atom displacement may represent different small domains of the material where the octahedra are twisted in opposite

(14) Shannon, R. D. *Acta Crystallogr.* **1976**, *32A*, 751.

(15) Anderson, M. T.; Greenwood, K. B.; Taylor, G. A.; Poeppelmeier, K. R. *Prog. Solid State Chem.* 1993, *22* (3), 197.

Table 2. Refined Atomic Coordinates for the Series $Pb_2(Sr/Ba)_2Cu_2MO_8X$[a]

	PbBaSbCl	PbSrSbCl	PbSrSbBr	PbBaNbCl	PbBaNbBr	PbBaTaCl	PbBaTaBr	PbSrTaCl	PbSrTaBr	$Pb_3BaTaCl$
Pb: (0.5,0.5,z)	0.1192(2)	0.1215(2)	0.1282(3)	0.12092(2)	0.1266(3)	0.1193(1)	0.1265(3)	0.1240(4)	0.1275(5)	0.1179(2)
B	1.14(6)	1.17(6)	1.59(10)	1.52(5)	1.01(10)	1.40(4)	1.07(9)	1.41(10)	1.46(16)	1.0(6)
Ba/Sr: (0.5,0.5,z)	0.3520(4)	0.3499(3)	0.3548(4)	0.3510(3)	0.3636(6)	0.3510(2)	0.3529(5)	0.3487(5)	0.3541(7)	0.3466(4)
B	0.84(10)	0.92(9)	1.12(12)	0.62(6)	0.56(15)	0.40(5)	0.52(15)	1.25(13)	1.31(20)	2.40(11)
M: (0,0,0.5) B	0.1(1)	0.3(1)	0(2)	0.60(6)	0.3(2)	0.51(5)	0.2(1)	0.2(2)	0.2(2)	0.52(10)
Cu: (0,0,z)	0.2217(3)	0.2282(3)	0.2349(4)	0.2218(2)	0.2271(4)	0.2213(1)	0.2283(4)	0.2283(4)	0.2354(7)	0.2229(3)
B	0.87(7)	0.58(6)	0.77(11)	0.92(5)	0.52(13)	0.71(4)	0.76(13)	0.81(11)	0.84(17)	0.60(7)
O1: (0,0.5,z)	0.2115(3)	0.2181(2)	0.2224(4)	0.2125(2)	0.2150(4)	0.2121(1)	0.2159(4)	0.2172(4)	0.2238(6)	0.2103(3)
B	1.36(7)	1.16(6)	1.12(10)	1.05(5)	1.03(11)	1.08(4)	0.8(11)	1.18(10)	0.73(14)	1.20(6)
O2: (0,0,z)	0.3752(3)	0.3760(5)	0.3775(2)	0.3775(2)	0.3794(5)	0.3766(2)	0.3785(5)	0.3803(7)	0.3835(10)	0.3752(4)
B	0.79.(9)	2.83.(12)	2.13(17)	1.20(6)	1.07(16)	1.14(5)	0.64(15)	2.53(19)	2.37(3)	1.70(10)
O3: (x,0.5,0.5)	0.0875(16)	0.1208(18)	0.1141(32)	0.0737(12)	0.0671(30)	0.0714(11)	0.0572(32)	0.1183(28)	0.122(4)	0.0746(20)
B	1.56(14)	2.12(16)	2.7(3)	1.74(10)	0.9(2)	1.46(9)	0.63(2)	1.58(2)	0.79(2)	1.73(16)
X: (0,0,0) B	2.41(12)	2.26(12)	1.42(17)	1.93(7)	1.8(3)	1.80(6)	0.99(18)	2.17(19)	1.6(3)	1.97(12)
χ^2	2.96	1.57	2.12	8.30	4.73	8.08	3.65	2.03	2.32	1.50
R_{wp} (%)	8.87	7.15	8.33	7.37	11.59	6.58	10.52	9.50	10.23	7.35
R_p (%)	6.91	5.51	6.33	5.29	7.84	5.19	7.46	7.21	7.69	5.61

[a] Esd values are given in parentheses; thermal parameter $B = 8\pi^2\langle u^2\rangle$ (Å^2).

Table 3. Derived Bond Lengths (in Å) from Powder Neutron Data, for the Series $Pb_2(Ba/Sr)_2Cu_2MO_8X$, M = Sb, Nb, and Ta and X = Cl and Br and for the Compound $Pb_3BaCu_2TaO_8Cl$

material	Pb−O1 × 4	Pb−X × 4	Ba/Sr−O1 × 4	Ba/Sr−O2 × 4	Ba/Sr−O3 × 4	Cu−O1 × 4	Cu−O2 × 1	M−O2 × 2	M−O3 × 4
$Pb_2Ba_2Cu_2SbO_8Cl$	2.4498(33)	3.3645(19)	2.960(5)	2.8225(9)	2.835(6)	1.9857(5)	2.403(6)	1.954(5)	2.0093(11)
$Pb_2Sr_2Cu_2SbO_8Cl$	2.4467(31)	3.3320(21)	2.8084(35)	2.790(1)	2.745(5)	1.9570(5)	2.275(8)	1.893(7)	2.0082(17)
$Pb_2Sr_2Cu_2SbO_8Br$	2.446(4)	3.4165(29)	2.842(6)	2.788(1)	2.739(9)	1.9635(9)	2.240(11)	1.912(10)	2.0040(28)
$Pb_2Ba_2Cu_2NbO_8Cl$	2.4436(22)	3.3730(14)	2.9373(31)	2.8275(7)	2.868(4)	1.9839(3)	2.433(4)	1.911(4)	1.9994(7)
$Pb_2Ba_2Cu_2NbO_8Br$	2.430(5)	3.4506(32)	2.959(8)	2.8389(16)	2.886(10)	1.9959(10)	2.409(10)	1.909(8)	2.0044(16)
$Pb_2Ba_2Cu_2TaO_8Cl$	2.4531(19)	3.3587(12)	2.9422(27)	2.8226(6)	2.8748(35)	1.9815(2)	2.432(4)	1.9301(30)	1.9966(6)
$Pb_2Ba_2Cu_2TaO_8Br$	2.440(5)	3.4502(30)	2.943(7)	2.8355(14)	2.922(10)	1.9939(9)	2.384(9)	1.928(8)	1.9972(15)
$Pb_2Sr_2Cu_2TaO_8Cl$	2.423(5)	3.3562(33)	2.813(6)	2.8007(22)	2.768(9)	1.9576(8)	2.344(13)	1.847(12)	2.0041(25)
$Pb_2Sr_2Cu_2TaO_8Br$	2.469(7)	3.422(5)	2.814(10)	2.7999(28)	2.743(13)	1.9624(14)	2.295(19)	1.854(16)	2.007(4)
$Pb_3BaCu_2TaO_8Cl$	2.4421(34)	3.3378(20)	2.896(5)[a]	2.8225(13)[a]	2.920(7)[a]	1.9806(6)	2.370(7)	1.946(6)	1.9929(12)

[a] The bond distances Ba/Pb−O1, −O2, and −O3 for this material.

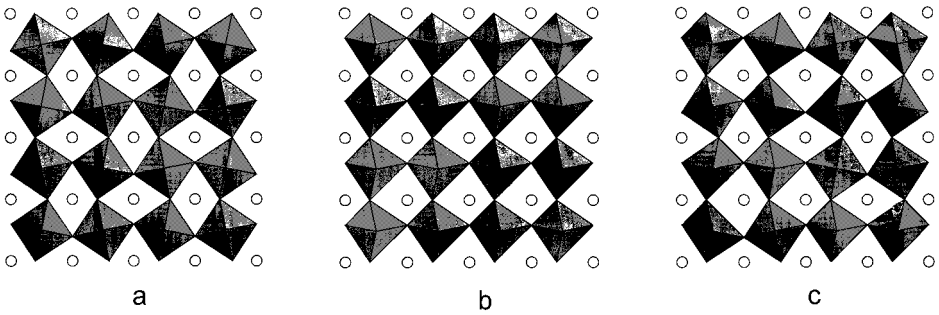

Figure 4. Schematic of the effect of displacing the O3 position from (0,0.5,0.5) to (0.1,0.5,0.5) on a layer of MO_6 octahedra: (a) a domain of oppositely aligned octahedra, (b) an area of distorted octahedra, and (c) a mixture of twisted and distorted units.

directions. Such a domain is shown in Figure 4a. Alternatively, the structure may consist of areas of similarly distorted octahedra (Figure 4b) or a mixture of twisted octahedra and distorted units (Figure 4c).

Partial replacement of barium by lead as in $Pb_3BaCu_2TaO_8Cl$ has very little effect on any of the structural parameters, though the coordination environment of the alkaline earth/lead site becomes more regular.

The $Pb_2(Ba/Sr)_2Cu_2MO_8X$ structure provides an important new addition to the family of layer cuprates, particularly in that it contains two unusual structural units, an ordered triple perovskite unit separated by a Pb_2X CsCl type layer. Through judicious choice of alkaline earth, halide, and pentavalent B cation it is possible to control various structural features of this material. In particular it is possible to produce a copper−oxygen environment close to that found in superconductors. However these phases, as synthesized with a copper oxidation state of 2+ and in plane Cu−O distances near 1.96 Å, would not be expected to exhibit superconductivity, and preliminary measurements show semiconducting behavior between room temperature and 4 K. With appropriate doping of this class of material with a small, low-valent ion it may be possible to increase the copper oxidation state and further reduce the in plane Cu−O distance to induce superconductivity. Such studies are in progress.

Acknowledgment. We thank the EPSRC for studentships for R.J.C and C.S.K. We also thank the EPSRC, DRAL, and the ILL for the provision of neutron beam time and technical assistance.

CM980609N